ELSEVIER

Catalysis Today 76 (2002) 103–112

CATALYSIS TODAY

www.elsevier.com/locate/cattod

FTIR study of the adsorption of single pollutants and mixtures of pollutants onto titanium dioxide in water: oxalic and salicylic acids

A.D. Weisz [a], L. García Rodenas [a], P.J. Morando [a,b], A.E. Regazzoni [a,b], M.A. Blesa [a,c,*]

[a] *Unidad de Actividad Química, Centro Atómico Constituyentes, Comisión Nacional de Energía Atómica, Avenida General Paz 1499, 1650 San Martín (Provincia de Buenos Aires), Argentina*

[b] *Instituto de Tecnología Jorge Sabato, Avenida General Paz 1499, 1650 San Martín (Provincia de Buenos Aires), Argentina*

[c] *Escuela de Posgrado, Universidad Nacional de General San Martín, 1650 San Martín (Provincia de Buenos Aires), Argentina*

Abstract

The use of ATR–FTIR to probe the adsorption of oxalic and salicylic acids, and of mixtures of both, onto TiO_2 (Degussa P-25) demonstrates the potential of the technique to characterise the evolution of the catalyst with time, including surface poisoning. Under equilibrium dark conditions, three surface species are formed by oxalate, and two by salicylate. Their stabilities, described by conditional Langmuir-type equilibria involving the dissociative, electroneutral adsorption of the acids H_2L, are at pH 3.7, 2.4×10^6, 3.0×10^4 and 3.0×10^3 mol^{-1} dm^3 for oxalic acid, and 2.9×10^5 and 9.1×10^3 mol^{-1} dm^3 for salicylic acid. The nature of the species is discussed in terms of their spectral features. The displacement of each acid from the surface by addition of the other one was followed also by ATR–FTIR. The results demonstrate that oxalate displaces totally chemisorbed salicylate, whereas salicylate displaces oxalate only partially. These results are explained by assuming competitive chemisorption onto two different surface sites, plus oxalate adsorption onto a site that exhibits negligible affinity for salicylate. Irreversible adsorption by partially oxidised products in the course of photocatalytic processes can therefore be assessed by ATR–FTIR.

Keywords: Photocatalysis; Titanium dioxide; Competitive adsorption; Carboxylic acids; FTIR

1. Introduction

The heterogeneous photocatalytic mineralization of organic pollutants in water involves a complex manifold of processes, all of which may effect the observed rates and photon efficiencies [1–4]. These processes are: (a) mass transport to and from the interfacial region; (b) kinetics of chemisorption of the pollutant (in many cases); (c) hole capture rates by adsorbed species; (d) kinetics of desorption of intermediates; (e) kinetics of conduction band electron injection; (f) kinetics of the (dark) chemical oxidation of intermediates; and (g) kinetics of the $^{\bullet}OH$ mediated oxidation pathway.

Heterogeneous photooxidation may be viewed as a chain reaction, in which only the first one electron

* Corresponding author. Present address: Unidad de Actividad Química, Centro Atómico Constituyentes, Comisión Nacional de Energía Atómica, Avenida General Paz 1499, 1650 San Martín (Provincia de Buenos Aires), Argentina. Tel.: +54-11-6772-7161; fax: +54-11-6772-7886.

E-mail address: miblesa@cnea.gov.ar (M.A. Blesa).

0920-5861/02/$ – see front matter
PII: S0920-5861(02)00210-9

oxidation step is necessarily linked to the capture of a hole. In the most favourable cases, all subsequent steps are thermal oxidation reactions (in photoelectrochemical setups, electron injection in the conduction band may be involved, giving rise to current multiplication). An oxidation length, Λ, may be defined as the ratio of the total equivalent number of one electron steps taking place to achieve the transformation of one pollutant molecule, to the number of holes consumed in the process [5]. For total mineralization,

$$\Lambda = \frac{n(4 - N^{av})}{h} \quad (1)$$

where n is the number of carbon atoms in the molecule of the pollutant, N^{av} the average carbon oxidation number, and h the number of holes consumed in the process; Eq. (1) is valid only for pollutants that do not contain heteroatoms.

The values of the oxidation length are especially affected by the dynamic behaviour of adsorbed intermediates. Easily oxidisable intermediates gives rise to high Λ values; intermediates reluctant to reaction with the dissolved oxidant, if easily desorbable, lead to incomplete mineralization or at least to temporary accumulation of intermediates in solution. Strongly adsorbed, oxidation-reluctant species lead to low oxidation lengths, low overall photooxidation rates and photon efficiencies, and, eventually, to surface poisoning.

In this paper, we report the results of an FTIR study of the adsorption on TiO_2 (Degussa P-25) in the dark of oxalic acid, salicylic acid, and mixtures of both. This technique has been used by several authors to probe the nature of the species formed by chemisorption of organic anions onto various metal oxides. In particular, Hug and Sulzberger [6], and Tunesi and Anderson [7] have made detailed spectroscopic studies of the species formed by adsorption of oxalic and salicylic acids onto titanium dioxide. A recent report [8] suggests that the formation of long-lived intermediates on the surface by salicylic acid photoelectrooxidation is inhibited by oxalic acid, probably by blocking some surface sites, thus preventing condensation reactions on the surface. Earlier, Regazzoni and co-workers [9,10] reported data on the affinity of both molecules for TiO_2; there it was assumed that adsorption–desorption was fast enough to permit the determination of affinity constants, more precisely the determination of the stability constants of the various surface complexes formed upon adsorption. Here, we report a more detailed study, in which the reversibility of ligand exchange is probed by using ATR–FTIR spectroscopy. The ATR mode permits to explore the interfacial region with minimum interference from the dissolved species. Previous work [11] has shown that dissolved species do not interfere in concentrations up to 10^{-3} mol dm^{-3}. The experiments in the dark described here provide an unambiguous answer as to the composition of the surface in contact with solutions of changing composition and, hence, it may be used to characterise surface poisoning under light.

The photocatalytic processing of oligocarboxylic acids is of importance in the nuclear industry, that employs these compounds as decontamination and chemical cleaning agents. Such a development is presently underway in our laboratories. Oxalate is an ubiquitous metabolic product, and its destruction by natural heterogeneous photocatalysis is of importance in aquatic systems.

2. Experimental

Titanium dioxide, Degussa P-25, was used as provided. The modal particle size is ca. 25 nm, and its BET specific surface area, determined from N_2 adsorption at 77 K, is 51.4 m^2 g^{-1}. The sample is mainly anatase, as indicated by PXRD; the content of rutile is less than ca. 10%.

All other reagents were analytical grade, and used as supplied. High purity water (18 MΩ cm) obtained from a Barnstead E-Pure apparatus was used in all experiments.

FTIR spectra were recorded using a NICOLET 560 instrument equipped with a liquid N_2 cooled MCT-A detector. A cylindrical ZnSe-ATR unit (length = 55 mm; diameter = 5 mm) or, alternatively, a horizontal ZnSe-ATR unit (area = 10 × 72 mm^2) was used. In both cases, the incidence angle was 45° and total number of reflections was 11. Both ATR elements were SpectraTech.

Layers of TiO_2 particles were deposited by placing variable amounts (50–150 μl) of TiO_2 suspensions (10–20 g/l) on the surface of the ATR crystal and evaporating to dryness at room temperature. The excess of TiO_2, in the form of loosely adhered particles, was

wiped off by a gentle rinsing with water. The coated crystal was mounted in an ATR flow-cell. Solutions were pumped from a 400 ml reservoir at a 7 ml/min flow rate; the total volume of the cell and tubing was ca. 12.0 ml.

Single pollutant adsorption experiments were performed as follows. The TiO_2-coated crystal was allowed to equilibrate with a ligand-free solution at a certain pH and ionic strength until the FTIR signal became stable, and a blank single-beam spectrum (I_0) was collected. Then, the concentration of the ligand of interest was fixed at a desired value, and the IR-absorption spectra ($\log(I_0/I)$) were recorded at 6–10 min intervals until signal amplitudes reached stable values (less than 2% change in 10 min). After recording the spectrum, the concentration of the ligand was increased, and the procedure repeated. Due care was taken to keep constant pH after each addition of ligand. The working temperature was $25 \pm 2\,^{\circ}C$. Spectral resolution was 4–8 cm^{-1}; each of the final spectra is the average of 500 scans. Base line corrections were made in order to eliminate minor fluctuations due to instrumental instabilities. Under these conditions, since the adsorbate concentration was always below ca. 1 mM, no appreciable IR signal was detected from solution species.

The reversibility of the adsorption process was explored by substituting the solution containing the ligand L_1, equilibrated with the film, by another one, in which the ratio $[L_2]/[L_1]$ was sequentially increased, while keeping $[L_1] + [L_2]$ constant. The FTIR–ATR spectra were recorded as before.

3. Results

Figs. 1 and 2 show the ATR–FTIR spectra of the TiO_2 films equilibrated with oxalic and salicylic acids, respectively, at pH 3.7. The maximum number of spectral components was assessed by singular value decomposition, assuming that the concentration dependence of each component is given by the Langmuir adsorption isotherm [11]. This leads to the identification of three and two independent surface complexes for oxalate and salicylate, respectively. The corresponding FTIR spectra are shown in Figs. 3 and 4.

The modelling of the concentration dependence using Langmuir-type adsorption isotherms gives the apparent stability constants shown in Table 1. Although the use of the Langmuir isotherm may be viewed as an oversimplification (see Section 4), it suffices to describe the experimental data excellently. The concordance with the Langmuir model indicates that the adsorption of the studied ligands is essentially

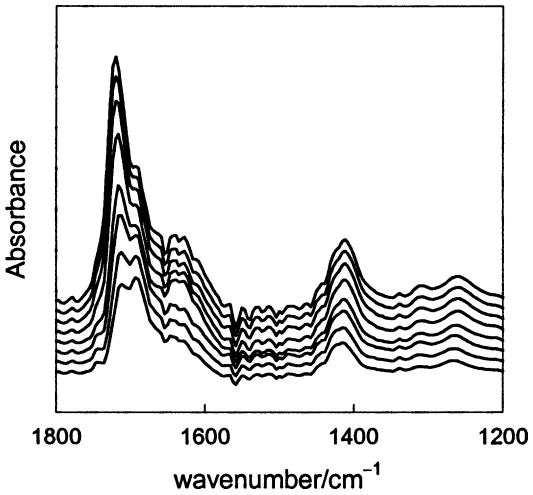

Fig. 1. ATR–FTIR spectra of a TiO_2 film in contact with solutions of increasing oxalic acid concentration. From bottom to top: 1.0×10^{-6}, 3.2×10^{-6}, 1.4×10^{-5}, 4.2×10^{-5}, 2.1×10^{-4}, 6.5×10^{-4}, 1.3×10^{-3}, and 2.0×10^{-3} mol dm^{-3}; pH 3.7.

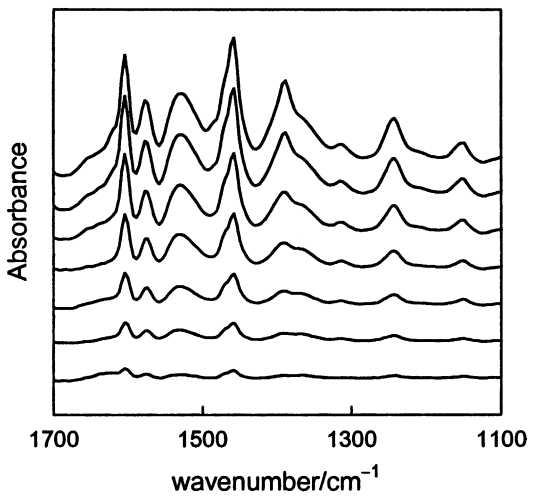

Fig. 2. ATR–FTIR spectra of a TiO_2 film in contact with solutions of increasing salicylic acid concentration. From bottom to top: 1.0×10^{-6}, 3.9×10^{-6}, 1.5×10^{-5}, 5.7×10^{-5}, 1.9×10^{-4}, 4.8×10^{-4}, and 1.0×10^{-3} mol dm^{-3}; pH 3.7.

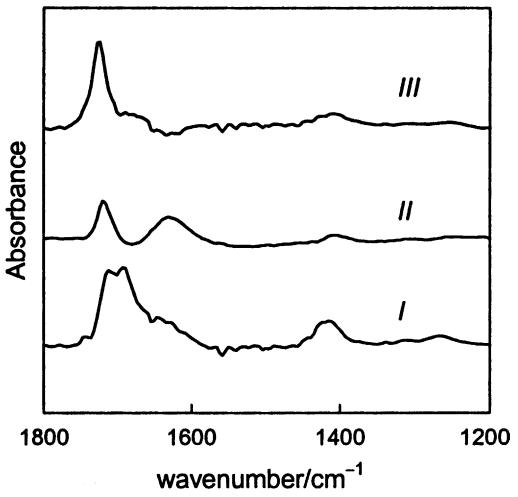

Fig. 3. Spectral components describing the concentration dependence of the ATR–FTIR spectra shown in Fig. 1; each component is the ATR–FTIR spectrum of a different oxalate surface complex formed onto TiO_2.

an electroneutral phenomenon, in which the acid H_2L adsorbs dissociatively, e.g.,

$$\equiv_{iv}Ti(OH)_2 + H_2L = \equiv_{iv}TiL + 2H_2O \quad (2)$$

In Eq. (2), ≡ indicates surface species, and the roman numeral subscript indicates the number of titanium coordination positions taken up by lattice oxo ions. It is further assumed that the overall coordination number of surface titanium atoms is always 6; the coordination shell is completed with species that are chemisorbed from solution (see Figs. 5 and 6). The pH dependence of $K_{L,i}$ values sustains the proton adsorption stoichiometry implicit in Eq. (2) [10,11].

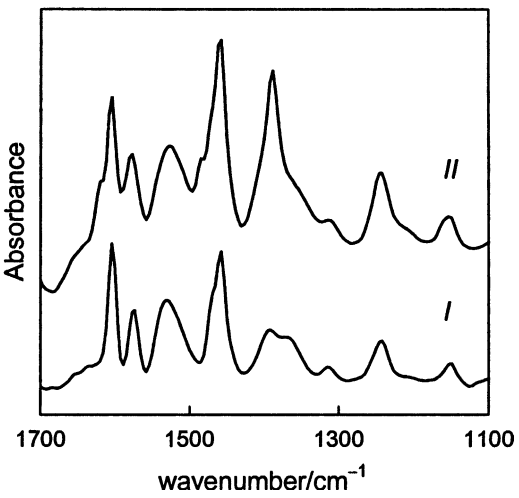

Fig. 4. Spectral components describing the concentration dependence of the ATR–FTIR spectra shown in Fig. 2; each component is the ATR–FTIR spectrum of a different salicylate surface complex formed onto TiO_2.

Table 1
Langmuir conditional stability constants for surface complexation by salicylate and oxalate at pH 3.7 and 25 °C

Adsorption mode	$\log(K_L/\text{mol}^{-1}\,\text{dm}^3)$	
	Oxalic acid	Salicylic acid
I	6.38	5.46
II	4.48	3.96
III	3.48	–

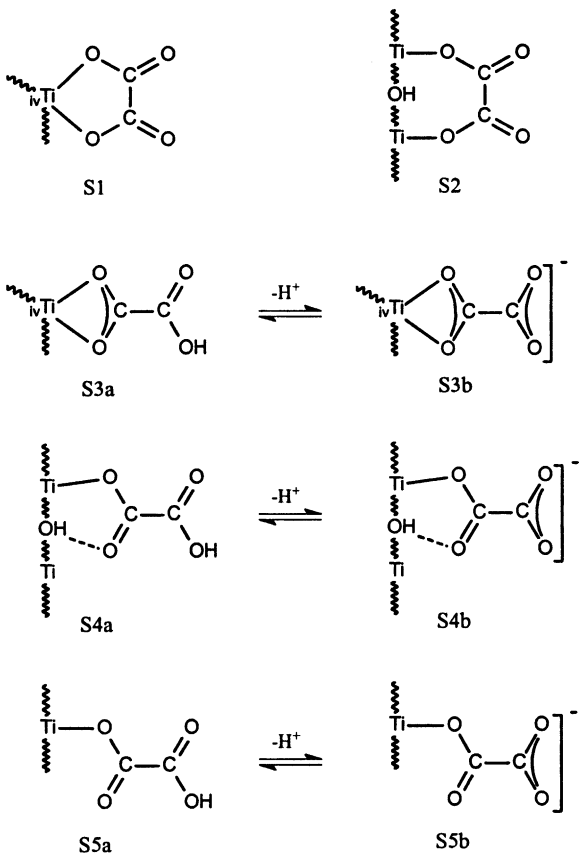

Fig. 5. Possible structures of the surface complexes formed by chemisorption of oxalic acid on TiO_2.

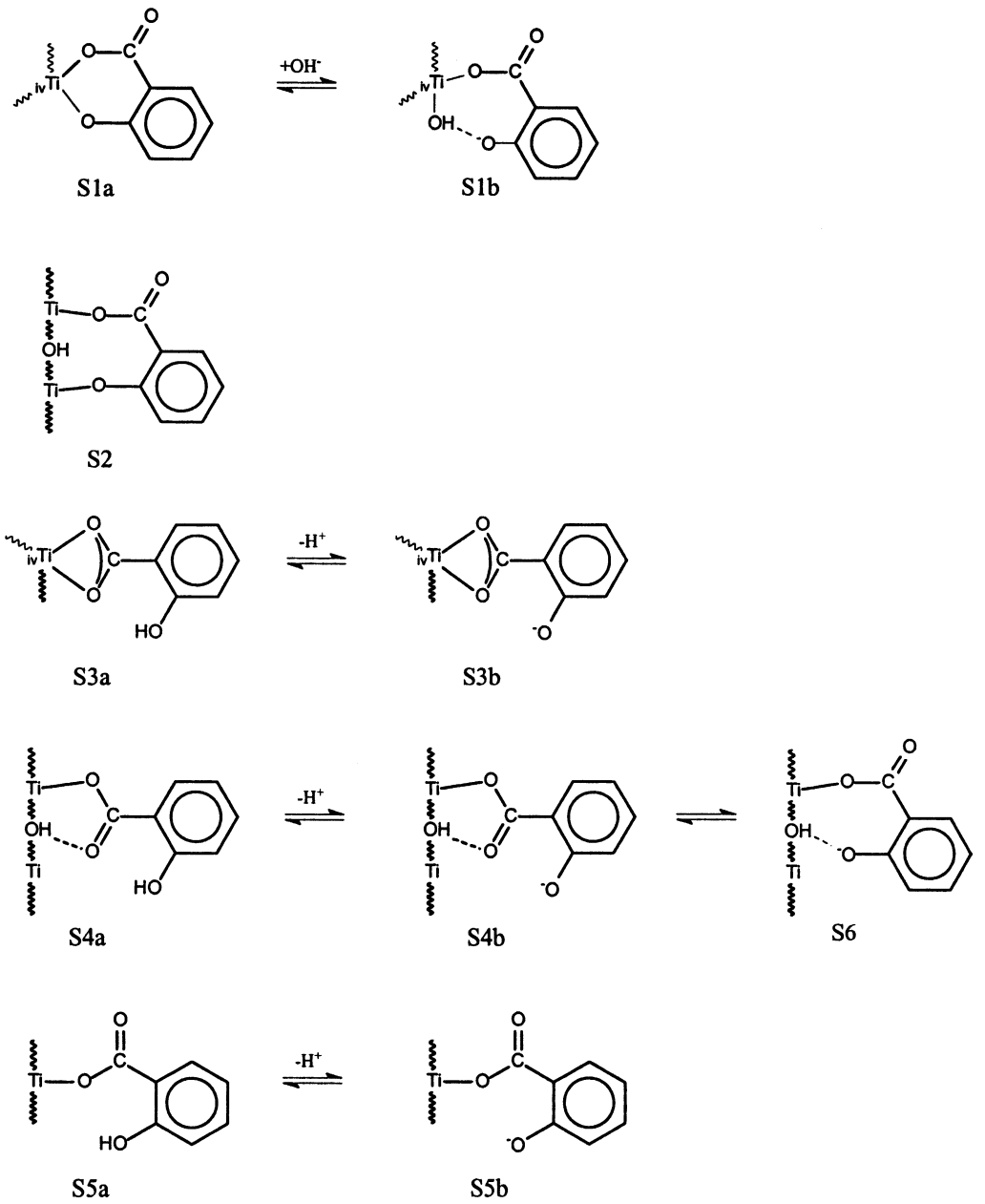

Fig. 6. Possible structures of the surface complexes formed by chemisorption of salicylic acid on TiO_2.

Band assignment for the main IR-absorption bands of the various surface complexes is summarised in Tables 2 and 3. The structure of the possible surface complexes (Figs. 5 and 6) is postulated from the positions and characteristics of the IR bands, especially those attributed to ν(C=O) and $\nu(CO_2^-)$. For oxalate, the spectroscopic evidence favours S1a as the most stable surface complex (adsorption mode I), S4b and/or S4a as the second more stable (adsorption mode II), and S5a as the less stable one (adsorption mode III),

Table 2
Band assignments for the different surface complexes formed by adsorption of oxalic acid onto TiO_2 at pH 3.7

Surface complex[a]			Assignment
I	II	III	
1712; 1692	1719	1726; ~1680 b	ν(C=O)
	1631		$\nu_a(CO_2^-)$
1415	1405	1409 b	ν(C–O) + ν(C–C)
1310 w	1305 w	1308 vw	$\nu_s(CO_2^-)$
1268 w	1252 w	1254 w	ν(C–O) + δ(O–C=O)

[a] b: Broad; w: weak; vw: very weak.

whereas for salicylate, it favours S1a as the most stable (adsorption mode I) and S4a (or eventually S2) as the less stable (adsorption mode II). In both cases, the most stable species is formed by chelation of a low coordination titanium atom (site C, in the terminology of Ref. [9]). For a detailed discussion of the band assignment and the proposed structures, the reader is referred to Ref. [11].

Figs. 7 and 8 explore the reversibility of oxalate and salicylate chemisorption. Spectra in Fig. 7 were recorded by increasing sequentially the [Ox]/[Sal] ratio in the aqueous solution in contact with a film pre-equilibrated with 10^{-3} mol dm^{-3} salicylate; the concentration ratio varied from 0.01 to 100 (square brackets represent the total, analytical, concentration of the ligands). The gradual disappearance of the bands centred at 1458 and 1389 cm^{-1} and the concomitant increase of that centred at 1417 cm^{-1} demonstrate that chemisorbed salicylate is reversibly replaced by oxalate; note also the shift of the

Table 3
Band assignments for the different surface complexes formed by adsorption of salicylic acid onto TiO_2 at pH 3.7

Surface complex		Assignment
I	II	
1680 bs[a]	1682 bs	ν(C=O)
1604; 1576	1605; 1578	ν(C–C)
1530	1527	$\nu_a(CO_2^-)$
1469; 1459	1483; 1460	ν(C–C)
1393; 1371	1389	$\nu_s(CO_2^-)$/δ(Ph–O–H)
1314	1313	ν(C–C)
1243	1244	ν(Ph–O)
1151; 1100; 1038	1153; 1099; 1036	δ(C–H) in plane

[a] Broad shoulder.

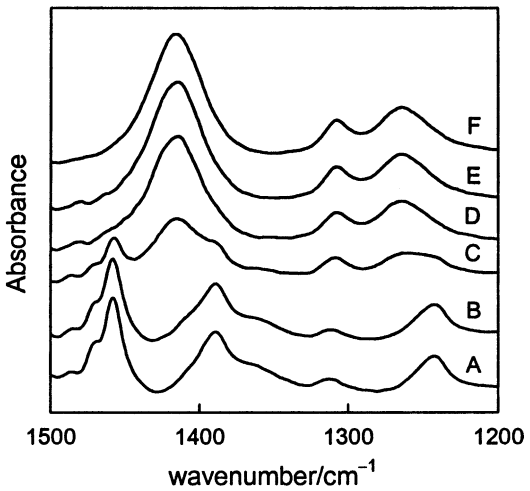

Fig. 7. ATR–FTIR spectra of a TiO_2 film pre-equilibrated with 10^{-3} mol dm^{-3} salicylate (A) in contact with solutions of varying [Ox]/[Sal] ratio: 0.01 (B), 0.1 (C), 1 (D), 10 (E), and 100 (F); pH 3.7.

1243 cm^{-1} band to higher wavenumbers. A simple model of equilibrated competitive adsorption, with only one adsorption mode for each ligand, using the adsorption constants derived before for the most stable modes ($K_{Ox}/K_{Sal} = 8.4$) describes qualitatively

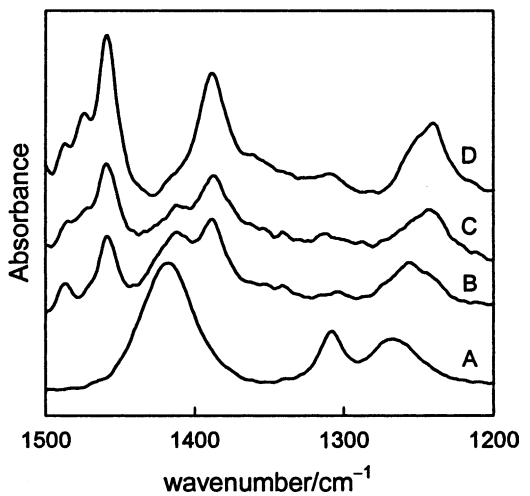

Fig. 8. ATR–FTIR spectra of a TiO_2 film pre-equilibrated with 10^{-3} mol dm^{-3} oxalate (A) in contact with solutions of varying [Sal]/[Ox] ratio: 100 (B), 1000 (C), and ∞ (D); pH 3.7.

the observed spectral changes. The time required to reach equilibrium was less than 20 min.

The three lower spectra in Fig. 8 correspond, from bottom to top, to a film that was pre-equilibrated with 10^{-3} mol dm^{-3} oxalate, and to the same film put in contact with solutions containing [Sal]/[Ox] ratios of 100 and 1000, respectively. The uppermost spectrum (D) corresponds to the oxalated film equilibrated with a solution containing 10^{-3} mol dm^{-3} salicylate and no added oxalate. The general features again correspond to a gradual substitution of chemisorbed salicylate by oxalate. This process is however incomplete, even after 5 h contact time, as revealed by the band at 1415 cm^{-1} in spectra B–D. It is worth stressing that equilibrium is attained in ca. 4 h, as judged by the evolution of the spectra. Fig. 9 shows sequential spectra corresponding to spectrum D in Fig. 8. Reasonably good isosbiestic points are found at ca. 1445 and 1410 cm^{-1}; the spectral changes in the lower range (1252 and 1239 cm^{-1}) are however indicative of a more complex sequence of events. Moreover, the different bands due to chemisorbed oxalate (1417, 1308 and 1268 cm^{-1}) are not removed at the same rate, suggesting that not all three surface complexes are displaced with the same rate; at least one is particularly resistant to salicylate substitution.

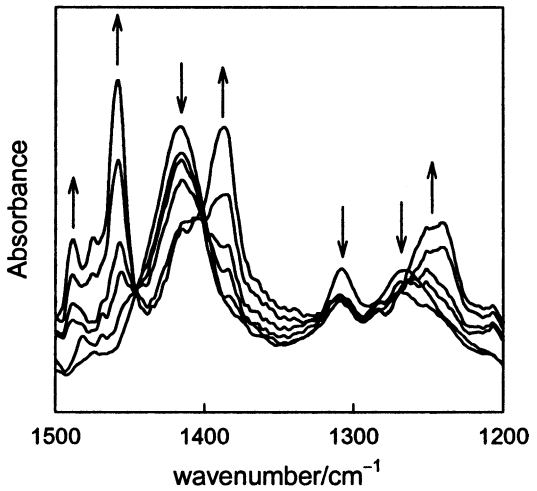

Fig. 9. Time evolution of ATR–FTIR spectra of a TiO_2 film pre-equilibrated with 10^{-3} mol dm^{-3} oxalate put in contact with a 10^{-3} mol dm^{-3} salicylate solution at pH 3.7; spectra were recorded at 0, 14, 71, 133, 232, and 264 min. The arrows indicate the sense of change of the main bands.

4. Discussion

In the dark, the interaction of titanium dioxide (Degussa P-25) with mixtures of oxalic and salicylic acids is adequately described by assuming equilibrated chemisorption onto the whole manifold of sites, in a time span ranging from a few minutes to a few hours. As discussed elsewhere [11,12], the adsorption of bidentate ligands from single component solutions may be described either by a two (or three) sites independent-adsorption model, or by a model of consecutive adsorption onto a single site. Intermediate cases, when more than two surface complexes are formed, can also fit the Langmuir description; this ambiguity arises from the intrinsic mathematical characteristics of the model. The spectroscopic evidence presented here points to two independent-adsorption modes, on different sites, in the case of salicylate, and either three independent-adsorption modes, or a combination of two consecutive modes on one site and another independent mode on a second type of site in the case of oxalate (cf. Figs. 3 and 4). The easy substitution of oxalate for salicylate (Fig. 7) demonstrates that the two types of sites involved in salicylate adsorption are also involved in oxalate adsorption. The more difficult, and incomplete, removal of oxalate by salicylate (Fig. 8), on the other hand, suggests that one of the three modes of oxalate adsorption is not sensitive to salicylate, as expected if the three oxalate surface complexes form by adsorption onto three independent sites.

The simple model of one ligand substituting the other, with a single value of K_{Ox}/K_{Sal}, albeit adequate for a qualitative description of the substitution of salicylate by oxalate (Fig. 7), is conceptually insufficient in view of the occurrence of different adsorption modes. In fact, it is unable to account for the lack of total oxalate substitution (Fig. 8). The information provided by FTIR–ATR is the ratio of the total surface concentrations of oxalate and salicylate complexes, Eq. (3), where $\{\}_i$ represents the surface density of the ith surface complex, which, for equilibrated competitive adsorption on independent sites, is given by Eqs. (4) and (5).

$$R_S = \frac{\sum_i \{\equiv \text{Ti–Ox}\}_i}{\sum_i \{\equiv \text{Ti–Sal}\}_i} \quad (3)$$

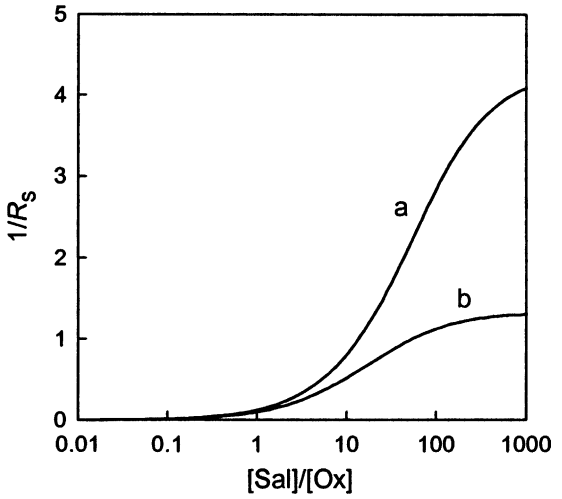

Fig. 10. Modelled equilibrium surface speciation as a function of [Sal]/[Ox] for two constant [Ox]: (a) 10^{-4} mol dm^{-3}; (b) 10^{-3} mol dm^{-3}; pH 3.7.

$$\{\equiv\text{Ti–Ox}\}_i = \frac{N_{S,i} K_{Ox,i}[Ox]}{1 + K_{Ox,i}[Ox] + K_{Sal,i}[Sal]} \quad (4)$$

$$\{\equiv\text{Ti–Sal}\}_i = \frac{N_{S,i} K_{Sal,i}[Sal]}{1 + K_{Ox,i}[Ox] + K_{Sal,i}[Sal]} \quad (5)$$

From these equations, using the stability constants presented in Table 1, and assuming that $N_{S,I} = N_{S,II} = N_{S,III}$, Fig. 10a and b can be drawn for [Ox] = 10^{-4} and 10^{-3} mol dm^{-3}, respectively. These figures describe adequately the changes in the experimental spectra shown in Figs. 7 and 8, even though the modelled conditions (i.e., constant [Ox]) are not identical to the experimental ones. If required, the latter conditions can also be modelled easily.

Next, we shall analyse the influence of surface speciation on the oxidation of the organic ligands upon illumination. In terms of adsorbed species, the general expression for the photooxidation rate is given by Eq. (6) [9], in which k_{ij} represents rate coefficients for irreversible hole capture by each of the jth ≡Ti–L$_i$ surface complexes (these coefficients are sensitive to the experimental conditions), and the last term accounts for •OH mediated oxidation reactions. Eq. (6) assumes that hole capture, or reaction with •OH lead to the final reaction products:

$$R = \sum_{ij} k_{ij}\{\equiv\text{Ti–L}_i\}_j + f([^{\bullet}\text{OH}], [\text{L}_i]) \quad (6)$$

In many cases, it is reasonable to assume that surface concentrations under light do not deviate much from their dark equilibrium values, because of the low photon fluxes and low photon efficiencies. Dark equilibrium surface speciation can therefore be used to interpret photomineralisation rate data (Eq. (6)). However, if the speciation is not known, no clear correlation can be established between the measured pollutant surface excess and the observed photooxidation rate [9,13].

Photooxidation of oxalate and salicylate is well documented. For oxalate, apparent first order kinetics has been reported in very different concentration ranges. Kosanic [14] reports that heterogeneous photooxidation in the micromolar range is mediated by an adsorption mode of affinity similar to that of the most stable mode found by us by ATR–FTIR (mode I), whereas Bryne and Eggins [15] report that oxalate photoelectrooxidation rates keep increasing with increasing substrate concentration, even in the millimolar range. Indeed, each of these sets of experiments explore the behaviour of different surface complexes. In agreement, a more complex behaviour has been reported recently for oxalate electrophotomineralisation [8], and the modelling presented in this paper suggests that the less stable surface complex is a better hole scavenger. In terms of our ATR study, at least two of the three adsorption modes are photoactive; close inspection of the original data suggests that all three may be involved, with non-negligible contributions of each one to the electrophotooxidation rate. On the other hand, zero order kinetics have been found in the photooxidation of salicylate at not too low concentrations and explained by assuming that the most stable surface complex is the one that mediates oxidation, acting as a hole trap [9]. These ideas are nicely supported by the present study, in terms of Eq. (6) and the surface speciation derived from our FTIR measurements. In the case of salicylate, it suffices to assume $k_{Sal,I} = 17.8\,s^{-1}$, and $k_{Sal,II} = 0$.

This conclusion is important to predict the behaviour of mixtures: whereas salicylate oxidation can be totally quenched by oxalate, by displacing the most stable complex, oxalate oxidation cannot be totally quenched by salicylate, as the oxalate unaffected adsorption mode (see above) shall always contribute to yield a non-zero rate.

The reaction product of oxalate photooxidation is CO_2, without accumulation of intermediates [8]. The ideal oxidation length for salicylic acid miner-

alization is 28, whereas the maximum value derived from electrophotooxidation experiments is ca. 8 [5]. Condensation reactions [16], which depend on the degree of coverage, may lead to the accumulation of rather unreactive intermediates on the photoelectrode surface [17], and may eventually lead to surface poisoning.

Our results demonstrate that the modelling of the photocatalytic oxidation of oxalate–salicylate mixtures should take into account equilibrated competitive adsorption on sites of different nature. Competitive adsorption is probably responsible for the inhibition of the formation of salicylate oxidation long-lived intermediates by oxalate [8]. In the modelling, it must also be taken into account that the [Ox]/[Sal] ratio may change with time due to (a) differences in the efficiencies of hole capture, and (b) non-reversible desorption of intermediates (in the case of salicylate); the first oxidation step of oxalate leads rapidly to CO_2.

The substrates used in this study are not representative of all classes of organic pollutants. Both oxalate and salicylate strongly chemisorb onto TiO_2, and previous work has suggested that photooxidation rates are linked to the surface concentration of the most stable surface complex [8,9]. Only at very low surface coverage (i.e., at very low bulk concentrations) participation of $^{\bullet}OH$ radicals may be important [8,17]. This is certainly not true in the case of molecules with low tendencies to displace surface $\equiv OH$ by ligand exchange [18]. The behaviour of methanol–carboxylate mixtures has been described recently [8]; in this case, the availability of $\equiv OH$ should perhaps be modelled also as a result of competition between ligand exchange and hole capture.

The use of Lagmuirian adsorption isotherms is certainly an oversimplification. In the pH spanned in this study, and at the majority of the explored ligand concentrations, the catalyst particles show negative electrophoretic mobility [19]. Current surface complexation models include adsorption modes that alter the charging state of the surface, thus rendering non-Langmuirian isotherms. Corrections based on electrostatic and lateral interactions, which are both a function of the degree of coverage, have been used by Regazzoni and co-workers [9,20,21]. These corrections are especially important to account for the pH dependency of the adsorption, from which most of the conditional nature of Langmuir-type constants arises. For our present purposes, the use of more elaborate models seems unjustified, as they require a rather large set of adjustable parameters.

Although it is understood that a detailed description of substrate adsorption is a pre-requisite for any modelling of photocatalytic oxidation, the kinetics of the adsorption–desorption process itself is an issue that has been left unattended; the information available in the literature is scanty and qualitative, and usually refers to adsorption from single component solutions [9,20–22]. Although there are limitations to the use of FTIR–ATR as a tool to study the kinetics of adsorption, our results are illustrative of the complexities of surface ligand-exchange kinetics: the replacement of salicylate by oxalate takes place in less than 20 min, whereas the reverse reaction occurs in about 4 h (Fig. 9); the origin of such different behaviours is unclear, but it is not related to differences in driving forces. These dynamic effects, which should greatly influence both photooxidation efficiencies and oxidation lengths, ought to be considered in any sound modelling of the photooxidation of single substrates and mixtures of pollutants. A detailed study of adsorption–desorption kinetics has now been undertaken in our laboratories.

Undoubtedly, ATR–FTIR is a valuable tool to characterise in detail the surface state in the course of dark substitution reactions, and there is no reason to limit it to dark or equilibrium conditions, as the evolution of illuminated surfaces can be equally followed. This is specially important in the cases in which complex pollutants are to be photodegraded, where robust, stagnant, intermediates are likely to be formed and lead to surface poisoning. Clearly, a detailed characterisation of the evolution of surface speciation will help in the understanding of the involved mechanisms and in the improvement of photomineralisation practical processes.

Acknowledgements

This work was supported by Grants from ANPCyT (PICT 06-06631), CONICET (PIP 4196) and CNEA (Program P-5, I&D). MAB, AER and PJM are members of CONICET, to which thanks are due for the Doctoral Fellowship awarded to ADW.

References

[1] D.F. Ollis, H. Al Akabi (Eds.), Photocatalytic Purification and Treatment of Water and Air, Elsevier, Amsterdam, 1993.
[2] O. Legrini, E. Oliveros, A.M. Braun, Chem. Rev. 93 (1993) 671.
[3] D. Bahnemann, P. Pichat, E. Pelizzetti, J. Cunningham, in: G. Helz, R. Zepp, D. Crosby (Eds.), Aquatic and Surface Photochemistry, CRC Press, Boca Raton, FL, 1994.
[4] C. Minero, G. Mariella, V. Maurino, E. Pelizzetti, Langmuir 16 (2000) 2632.
[5] P. Mandelbaum, S.A. Bilmes, A.E. Regazzoni, M.A. Blesa, Solar Energy 65 (1999) 75.
[6] S. Hug, B. Sulzberger, Langmuir 10 (1994) 3587.
[7] S. Tunesi, M.A. Anderson, Langmuir 8 (1992) 487.
[8] M.E. Calvo, R.J. Candal, S.A. Bilmes, Environ. Sci. Technol. 35 (2001) 4132.
[9] A.E. Regazzoni, P. Mandelbaum, M. Matsuyoshi, S. Schiller, S.A. Bilmes, M.A. Blesa, Langmuir 14 (1998) 868.
[10] A.D. Weisz, A.E. Regazzoni, M.A. Blesa, Solid State Ionics 143 (2001) 125.
[11] A.D. Weisz, Ph.D. Dissertation, University of Buenos Aires, Buenos Aires, Argentina, 2001.
[12] M.A. Blesa, A.D. Weisz, P.J. Morando, J.A. Salfity, G.E. Magaz, A.E. Regazzoni, Coordin. Chem. Rev. 196 (2000) 31.
[13] J. Cunningham, G. Al-Sayyed, J. Chem. Soc., Faraday Trans. 86 (1990) 3935.
[14] M.M. Kosanic, J. Photochem. Photobiol. A 119 (1998) 119.
[15] J.A. Bryne, B.R. Eggins, J. Electroanal. Chem. 457 (1998) 61.
[16] M.E. Calvo, S.A. Bilmes, R.J. Candal, Presented at XII Congreso Argentino de Fisicoquímica y Química Inorgánica, San Martín de los Andes, Neuquén, Argentina, April 2001.
[17] P. Mandelbaum, Ph.D. Dissertation, University of Buenos Aires, Buenos Aires, Argentina, 1999.
[18] P. Mandelbaum, A.E. Regazzoni, S.A. Bilmes, M.A. Blesa, J. Phys. Chem. B 103 (1999) 5505.
[19] M. Matsuyoshi, L.A. García Rodenas, M.A. Blesa, Unpublished result.
[20] R. Rodríguez, M.A. Blesa, A.E. Regazzoni, J. Colloid Interf. Sci. 177 (1996) 122.
[21] M. Matsuyoshi, R.T. Gettar, M.A. Blesa, A.E. Regazzoni, Presented at 10th International Conference on Colloid and Interface Science, Bristol, UK, July 2000.
[22] S. Tunesi, M.A. Anderson, J. Phys. Chem. 95 (1991) 3399.